



## Verification for the accuracy of evaluation index for tsunami simulation

Y. Eguchi<sup>(1)</sup>, Y. Shigihara<sup>(2)</sup>, T. Tada<sup>(3)</sup>

<sup>(1)</sup> Student, National Defense Academy, Japan, em58045@nda.ac.jp

<sup>(2)</sup> Associate professor, National Defense Academy, Japan, shigi@nda.ac.jp

<sup>(3)</sup> Associate professor, National Defense Academy, Japan, tada@nda.ac.jp

### **Abstract**

The 2011 Tohoku earthquake made gigantic tsunami, and a large area in the Pacific coast of Tohoku was inundated. The data of wave profiles, inundated area, and the tsunami heights surveyed by researchers were used for confirming the accuracy of numerical simulation. However, few studies on the characteristic of index for the accuracy of tsunami simulation were conducted.

This study aimed to confirm the characteristic of proposed evaluation index for tsunami simulation. We performed numerical simulation of the 2011 Tohoku tsunami in Sendai plain by using the Finite Difference Method, and investigated trend of the difference between simulated tsunami heights and observed one at each point. Several factors in numerical simulation were changed, such as fault model, the Manning's roughness coefficient and the spatial grid resolution. We identified what change of factor improved numerical simulation and which index was accurately linked the change.

Comparison between the observed inundation area and that of the numerical simulation showed that the simulated tsunami heights tended to be overestimated as the distance from shoreline increases, especially 1500 m over. Although this simulation result seemed to be made by not sufficient decline of roughness coefficient, the effects of the fault model and the spatial grid resolution were actually larger than the effect of the bottom roughness. In addition, the scale of these effect was different by the location, therefore intentional selection of the trace could improperly improve evaluation index for tsunami reproducibility.

*Keywords: the 2011 Tohoku tsunami, tsunami simulation, evaluation index*



## 1. Introduction

The tsunami that occurred in the 2011 Tohoku earthquake caused inundation damage over a wide area in the Pacific coast of eastern Japan. Researchers immediately started post tsunami survey after the event and collected a large amount of data, such as GPS and trace of the tsunami run-up and inundation heights, from Hokkaido to Kanto region. This was the real data from run-up of tsunami, unlike hydraulic experiments and analytical solutions.

The tsunami data compiled from the survey have been used in various studies to improve the accuracy of tsunami simulation. Montoya et al. (2016) [1] evaluated the accuracy of the two kind of tsunami models and the contribution of the spatial grid resolution to the results by comparing with the run-up limit. Baba et al. (2015) [2] evaluated the effects of dispersive tsunami on inundation height and area by using traces in Miyagi Prefecture. In these studies, it was analyzed the factors that can make the difference in simulation result compared to the trace data. However, there have not been many studies about the indexes used for evaluation of reproduction, so it is unclear in what cases the index value improved against the real situation.

In this study, we attempted to confirm the influence on the inundation height by changing the fault model, the spatial grid resolution, and the Manning's roughness coefficient, and examined how the index value changed with these factors. In particular, the effect level of each of the above factors on the inundation height were organized and compared.

## 2. Data

A lot of data on trace heights were collected over a wide area from Hokkaido to Kanto region after the earthquake. The trace data also have been collected in Sendai, where the tsunami simulation was performed in this study. However, some traces showed unnaturally high data plotted at distances from the shoreline. Tada et al. (2018) [3] classified these by the following criteria and selected traces that were suitable for comparison with tsunami simulation using the Nonlinear Shallow Water Equations (NSWE).

Inundation height on broken branches [IB]: Inundation height of broken trees near the coastline, debris on trees and steel towers, etc., which were suspected of splash on coastal dikes.

Building front [IF]: Inundation height at the front of a relatively tall building, which was considered to have remained higher than the surrounding area due to reflections and collisions of large debris.

Trace affected by reflection [RR, IR]: Unusually high runoff (RR) at coastal slopes and steep slopes of the road embankment, and higher inundation depth (IR) than the surroundings that occurred in the direction of wave incidence due to reflections at these slopes.

Trace influenced by river [IC, RC]: Inundation height (IC) and run-up height (RC), which were likely to be affected by the river and its surrounding topography, or by the tsunami going up the river channel faster than the surrounding land.

Unreliable trace [IX, RX]: the reliability was low or difficult to use for comparison due to unclear trace, the measured heights and the comments by surveyors were clearly inconsistent, or the inundation depth was negative value and the reliability was low

Undisturbed measurements [IN, RN]: Measured height that were considered to reflect the state of flow without being affected by obstacles and irregularities of fine terrain were regarded as undisturbed measured height. It corresponded to the remaining the data, excluding data identified as other classifications from all data.

In this study, the undisturbed trace height data IN and RN were used for comparison with the simulation results.

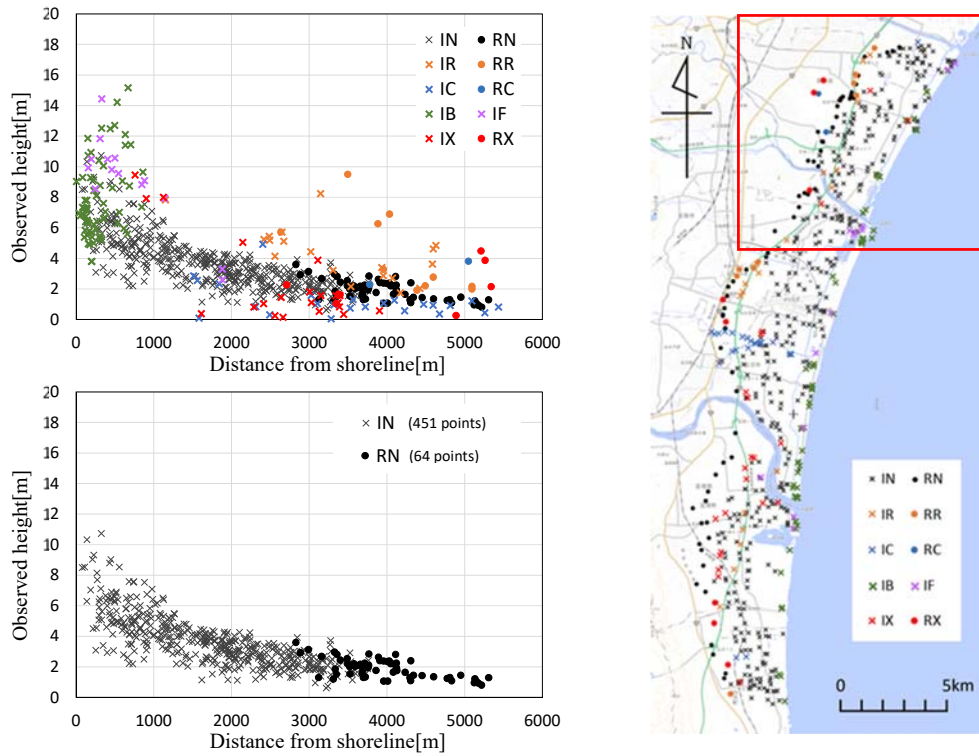


Fig. 1 – (a) Trace distance from shoreline and distribution of trace heights classified into each type.

(b) The distance of the traces used in this study from the shoreline and the distribution of the trace heights.

(c) Distribution of places where each type of trace was recorded. Traces in the simulation area of 5m grid used for comparison this time are within the red frame.

### 3. Method

We used the NSWE including the bottom friction and the advective terms. The continuation equation (1) and the equation of motion of (2) and (3) [4] were used as the governing equation:

$$\frac{\partial \eta}{\partial t} + \frac{\partial M}{\partial x} + \frac{\partial N}{\partial y} = 0 \quad (1)$$

$$\frac{\partial M}{\partial t} + \frac{\partial}{\partial x} \left( \frac{M^2}{D} \right) + \frac{\partial}{\partial y} \left( \frac{MN}{D} \right) + gD \frac{\partial \eta}{\partial x} + \frac{gn^2}{D^3} M \sqrt{M^2 + N^2} = 0 \quad (2)$$

$$\frac{\partial N}{\partial t} + \frac{\partial}{\partial x} \left( \frac{MN}{D} \right) + \frac{\partial}{\partial y} \left( \frac{N^2}{D} \right) + gD \frac{\partial \eta}{\partial y} + \frac{gn^2}{D^3} N \sqrt{M^2 + N^2} = 0 \quad (3)$$

where,  $M$ ,  $N$  are the line discharge flux in the  $x$ ,  $y$  direction respectively,  $g$  is the gravitational acceleration,  $n$  is the Manning's roughness coefficient,  $\eta$  is the wave height,  $h$  is the still water depth, and  $D (= \eta + h)$  is the total water depth.

For the tsunami simulation, the Staggered Leap-frog finite difference method [5] based on the nonlinear long-wave theory was used, and the spatial grid resolution was set from the largest domain of 1215 m (all over East Japan) to the 6th domain of 5 m (Sendai plain). The domains were connected by the two-way nesting method. The simulation time was 120 minutes.

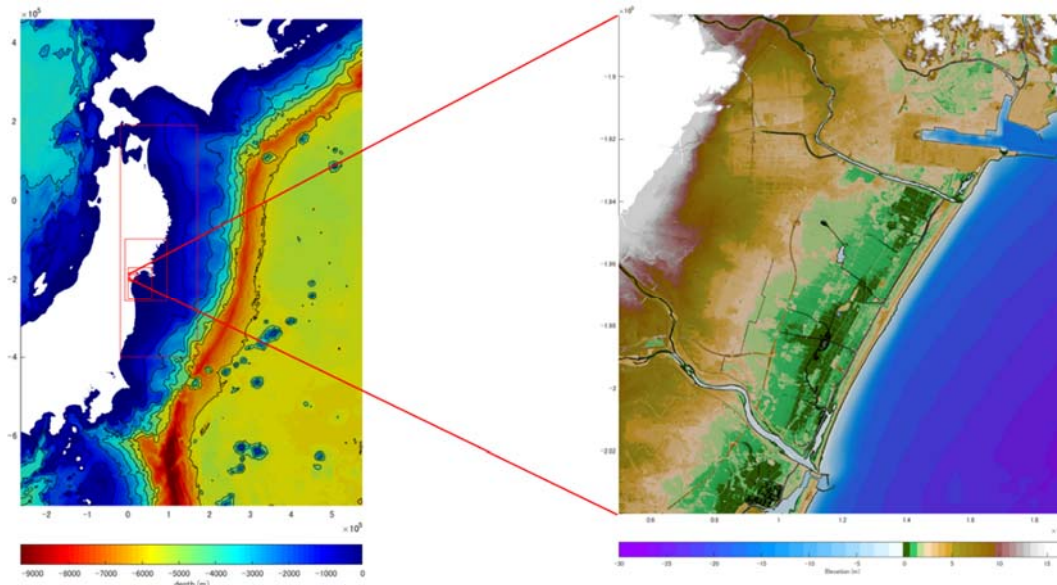


Fig. 2 –1215 m grid area (left) and 5 m grid simulation area. The areas of 405 m, 135 m, 45 m, and 15 m connected 1215 m area were indicated by the red frame in the left figure.

Fujii et al. (2011) [6] and Tohoku University (2011) [7] were used for the fault model that was the initial condition of the tsunami. Fujii model (FS model) was proposed based on the inversion of tsunami waveforms. The Tohoku University model (TU model) was proposed as a fault model to reproduce the inundated area recorded by TTJS group [8]. Comparing the waveforms with the GPS wave gage offshore Sendai, the TU model had a shorter wavelength and the FS model had a larger amplitude than the observed one. (Fig. 3)

On the other hand, setting the roughness coefficient based on land use was expected to improve the accuracy of tsunami simulation. Kotani et al. (1998) [9] attempted to improve the accuracy of damage prediction by setting the roughness coefficient according to land use. Roughness map based on land use were also applied in tsunami simulation by the government of Japan. In Sendai, the Cabinet Office has released roughness maps based on land use before the 2011 tsunami event.

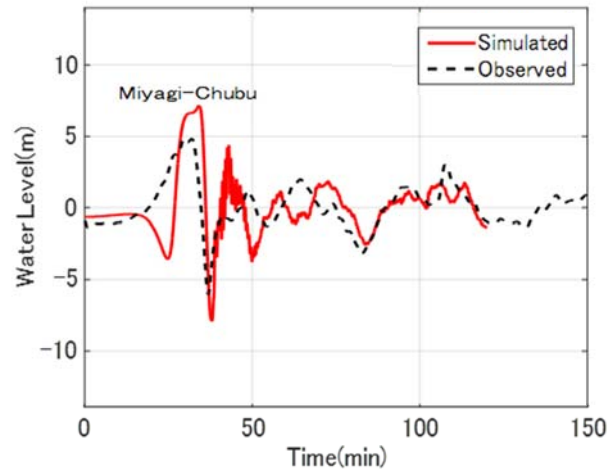
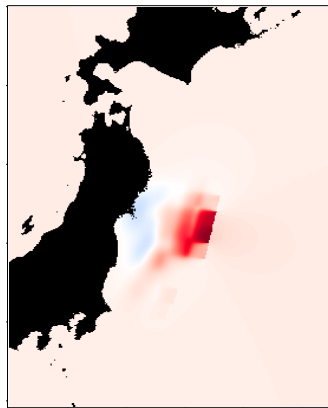
The roughness map of Sendai, using in this study, distributed coastal forests ( $n = 0.030$ ), field ( $n = 0.020$ ), and urban areas ( $n = 0.035$ ). In general, tsunami simulation is conducted with  $n = 0.025$ , which is equivalent to be sand diameter of 2 cm, or roughness coefficient based on land use. In addition to the two roughness application, we tested the tsunami simulation with  $n = 0.035$ , which was the largest roughness value in the roughness map of Sendai.

We also evaluated the difference due to the spatial grid resolution of the simulation. Montoya et al. (2016) suggested that in order to predict run-up heights and inundation limits, making the grid resolution fine beyond 30 m did not result in any significant change in the simulation results. On the other hand, the simulation of the Nankai Trough great tsunami by the Cabinet Office was simulated with the map of 10m grid size and the results were published as the hazard maps along Pacific coast of Japan. Comparing the preliminary report with 50 m mesh, in some area, the tsunami height changed up to 8 m. Therefore, the influence of the spatial grid resolution on the calculation results was examined.

To evaluate the accuracy of the tsunami simulation, the following index by Aida (1978) [10], which was one of the indexes for evaluating the spatial reproducibility of the trace heights of the past tsunami and the simulated heights. The geometric mean  $K$  and the geometric standard deviation  $\kappa$  were used. This was often used as one of the studies on the reproducibility of the tsunami simulation



The FS model



The TU model

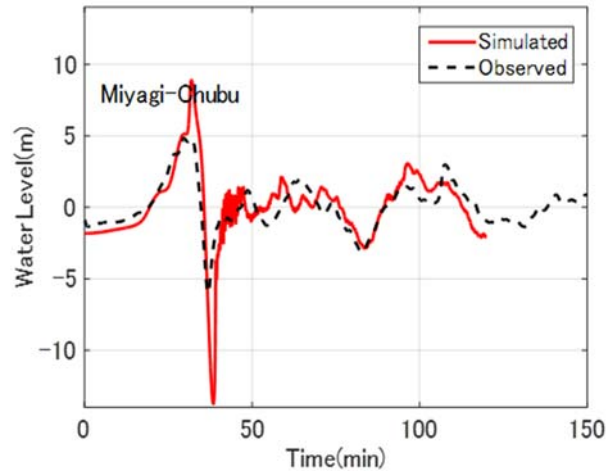
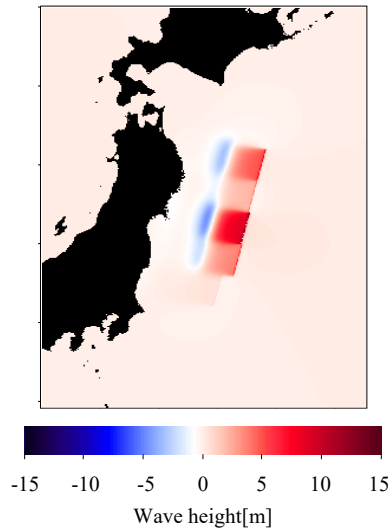


Fig. 3 –Comparison of the water level at  $t = 0$  in each fault model (left). The observed and simulated tsunami in GPS wave gage of central Miyagi (right)

$$\log K = \frac{1}{n} \sum_{i=1}^n \log K_i \quad (4)$$

$$\log \kappa = \left[ \frac{1}{n} \left\{ \sum_{i=1}^n (\log K_i)^2 - n(\log K)^2 \right\} \right]^{\frac{1}{2}} \quad (5)$$

where,  $n$  is the number of trace,  $R_i$  is observed height,  $H_i$  is simulated height of  $i$ -th trace, and  $K_i (= R_i / H_i)$  is fraction of two heights. The Japan Society of Civil Engineers (2012) [11] has determined that  $0.95 < K < 1.05$  and  $\kappa < 1.45$  are appropriate for these indexes.

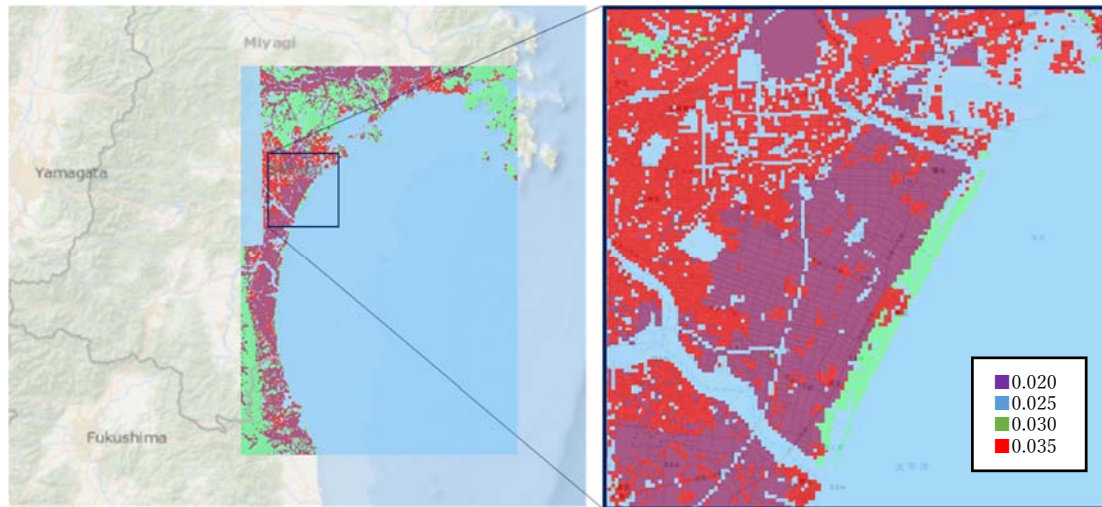


Fig. 4 –The roughness map based on the land use we applied this time. The spatial grid resolution of the published data was 50 m, and we changed the grid resolution to fit the simulation.

## 4. Result and Discussion

### 4.1 Simulated and observed heights

Fig. 5 shows comparison of the simulated and observed heights. The simulated heights were generally estimated to be greater than the observed heights. If  $K$  is less than 1, the calculated tsunami height is overall underestimated than that of the observation. In both model result, most of simulated heights were larger than observed heights, and  $K$  were expected smaller than 1, especially in the FS model.

$K = 0.62$ ,  $\kappa = 1.75$  for the FS model,  $K = 0.79$ ,  $\kappa = 1.41$  for the TU model, it suggested the TU model had better reproducibility for both indexes. On the other hand, although the simulated heights in the FS model were larger than the TU model in most trace location, the extent was not uniform in the whole area. Around the observed heights of 2 m to 5 m, the simulated heights of the FS model were distributed around 4 m to 7 m, however, that of the TU model were distributed around 2 m to 4 m. Also, the other range of the observed heights, simulated heights slightly changed in two type of fault model.

Although the whole reproducibility and the tendency could be seen in Fig. 5, to evaluate the reason of the difference in the reproducibility by trace location was difficult. Therefore, we tried to find the reason and correlated physical value for change in inundation situation.

### 4.2 Fault model

Focusing on the spatial distribution of the difference between the observed heights and the simulated heights for each trace location is able to find common and different characteristics among the two type of fault models. The difference between the observed height and the simulated height is plotted at the trace location. (Fig. 6) The simulated heights in the two type of fault models are almost the same in the coastal area but quite different in the inland area. The tsunami generated by the two type of fault models had different characteristics in amplitude and wavelength in offshore. (Fig. 3) However, the contribution to the inundation height during the run-up process varied from place to place.

The reason for the difference in the inundation heights of the FS model and the TU model was examined by comparing their simulation results. Fig. 7 shows the line discharge flux distribution in tsunami run-up. The line discharge flux is expressed by the product of flow velocity and water depth. When the tsunami run-up



process was viewed over time, the velocities of the surge front of tsunami were always maximum and gradually decreased. On the other hand, the water depth was higher in coastal areas except for the local topography such low-lying as depressions. The line discharge flux clearly showed where the tsunami was moving up.

The line discharge flux in tsunami run-up process showed clearly the reason for the different inundation heights in the two type of fault model. After the peak of the first wave had passed though the shoreline, the line discharge flux would become smaller. However, especially in the FS model, the much line discharge flux was kept in the south side of the Nanakita River in spite of the decrease of flow from shoreline. To cause such situation, flow supply was required except from the shoreline. Therefore, we investigated the variation of tsunami in run-up process, in the north side of the Nanakita River, the tsunami reflected at a slightly high area in the industrial area and head toward south. In other words, on the south side of the Nanakita River, the simulated tsunami run up from the Nanakita river in addition to from shoreline. This additional flow from the Nanakita River correlated with difference of the inundation heights in the two type of fault model. In other area, where the FS model showed larger inundation heights such as the road embankment and the Sendai port, increase of the line discharge was similarly confirmed.

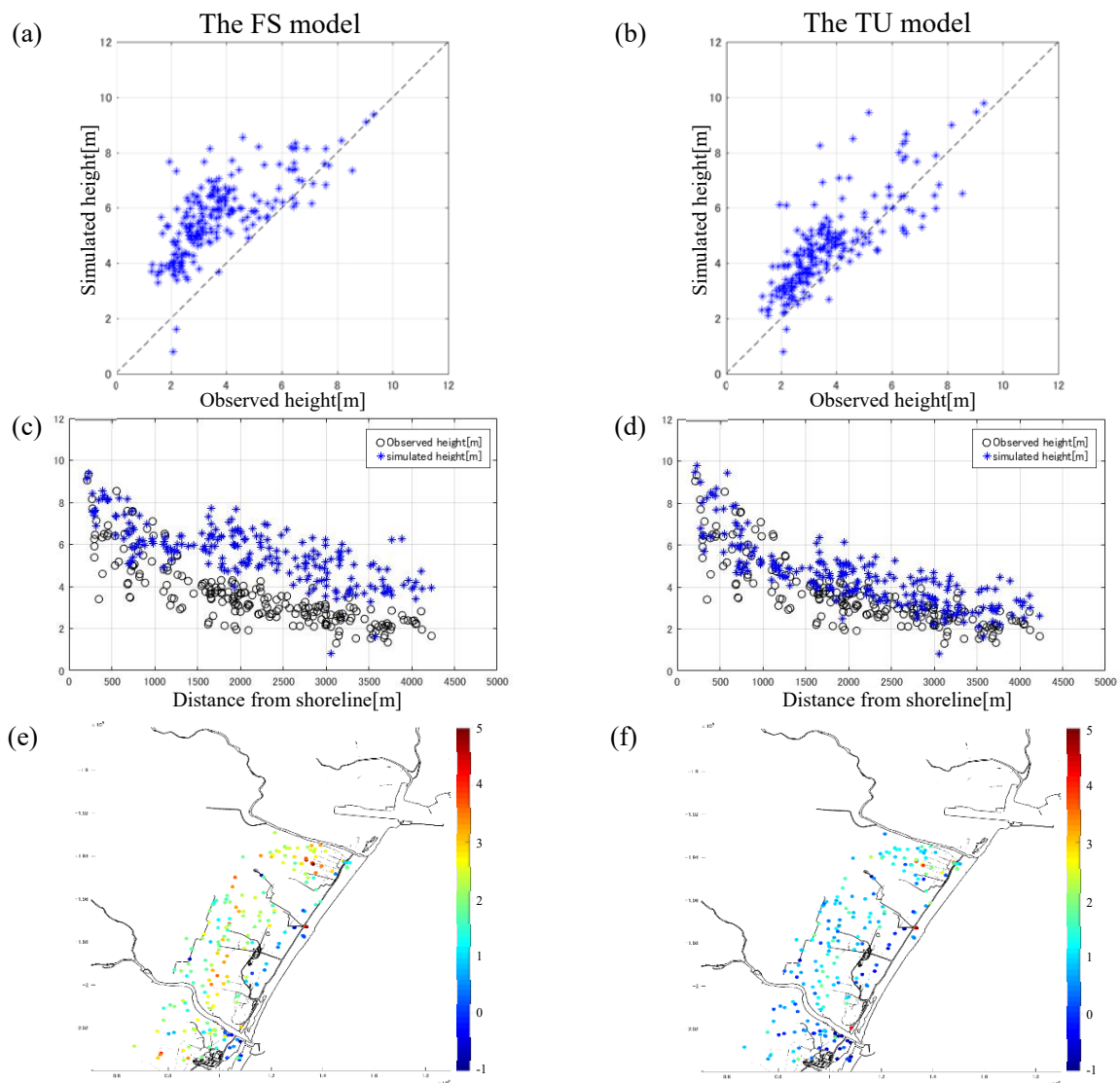


Fig. 5 – (a), (b) Comparison of observed and simulated heights in the two type of the fault model. (c), (d) Distance from shoreline and comparison of observed heights and simulated heights. (e), (f) Distribution of difference “simulated height” - “Observed height” at each trace location.



From the above discussion, a locally large flow generated by the local topography such as rivers or road embankments increase the inundation height. When plotted by the distance from the shoreline, the FS model appears to have a smaller attenuation at first glance, but since the roughness is the same, it is due to the effect of a locally large flow.

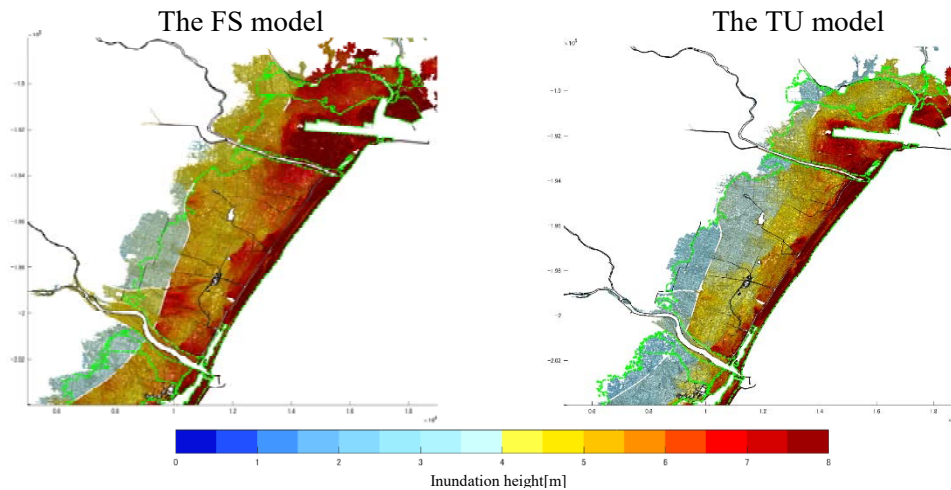


Fig. 6 –Distribution of inundation heights in each fault model. The observed inundation area is indicated by a yellow-green line.

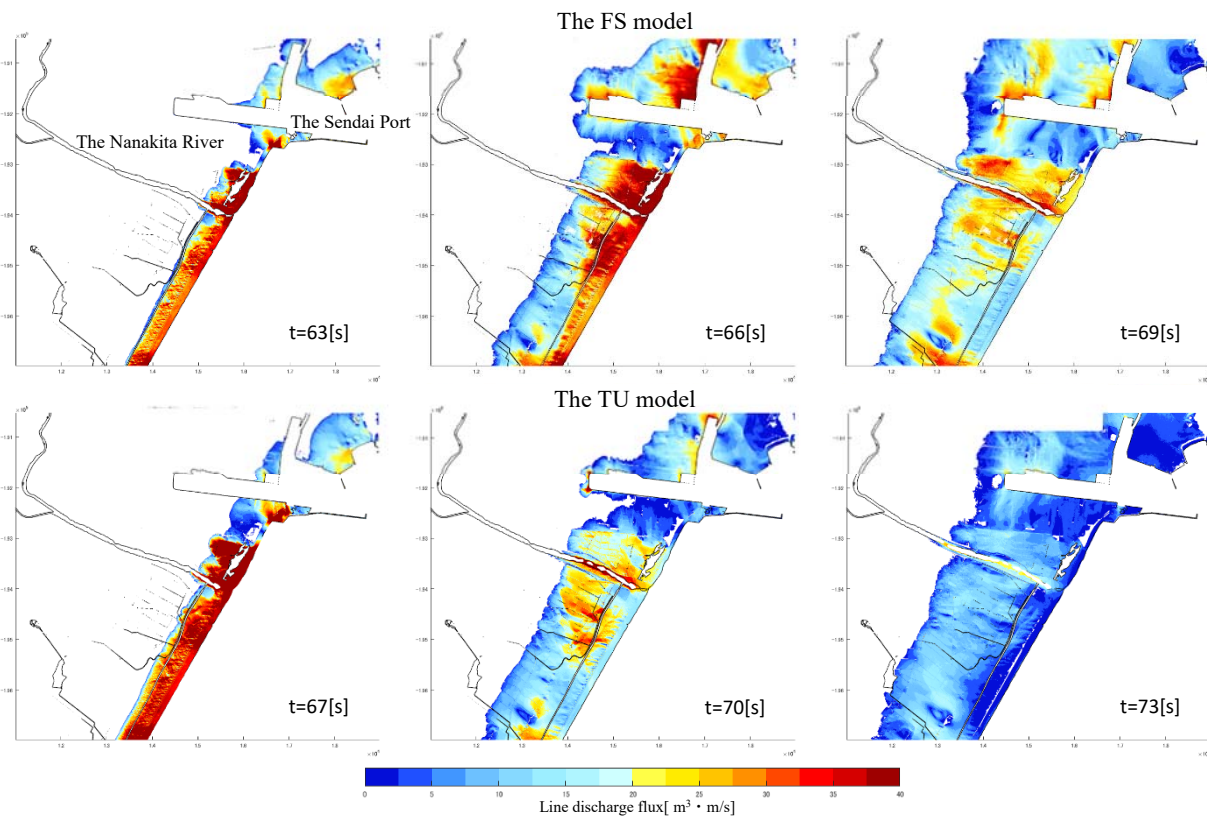


Fig. 7 –Changes in the line discharge flux in each fault model. Since the arrival times of tsunami were different, the snapshot used for comparison was decided for the situation of tsunami. The simulated tsunami in the TU model had the large first wave amplitude, but that in the FS model had the longer wavelength and ran up to the inland.



Also, if the location of the trace is selected and limited by itself, the accuracy of the simulated results may be unexpectedly improved. Error of the reproducibility of observed inundation was not evenly distributed, but good and bad area locally existed. For example, if only the location of trace heights along the coastal lines and the run-up points were used,  $K$  and  $\kappa$  will be improved, and it will appear as if the reproducibility is good

#### 4.3 Roughness coefficient

Next we compared the inundation heights by changing the roughness coefficient. First, roughness map based on land use published by the Cabinet Office before the 2011 tsunami event was applied. We compared this simulation result with the case where the roughness coefficient fixed at  $n = 0.025$ . (Fig. 8(a)) When roughness coefficient was set to  $n = 0.025$ ,  $K = 0.79$  and  $\kappa = 1.41$ , whereas when roughness model based on land use,  $K = 0.79$  and  $\kappa = 1.42$ . Difference of the simulated heights in two type of roughness coefficient condition was less than 1 m, which was much less than comparison of the two type of the fault model discussed in the previous section. Also, Fig. 8(a) indicated that the difference in inundation heights had no correlation with the topography and the roughness coefficient.

This suggested that in Sendai, the tsunami inundation simulation in which the roughness coefficient was based on land use was not much different from that in which the roughness coefficient was set to  $n = 0.025$  in the whole area.

However, we couldn't conclude that the  $n = 0.025$  was proper for the roughness coefficient with only this result. If roughness coefficient had little effect on the tsunami run-up process, change of roughness coefficient should make little difference in simulation result. Therefore, we compared the simulated result with the case where the largest value of  $n = 0.035$  in this roughness model was applied to the whole simulated area in addition.

The inundation height applied  $n = 0.035$  to the land roughness was compared with the case of  $n = 0.025$  (Fig. 8(b)). When the roughness coefficient was set to  $n = 0.035$ ,  $K = 0.81$  and  $\kappa = 1.38$ , and the index value was slightly improved. When the roughness coefficient was set to  $n = 0.035$ , the inundation height increases near the coast, while when the roughness coefficient was set to  $n = 0.025$ , the inundation height increases inland. However, this difference did not significantly affect the tsunami simulation, because the difference in the inundation height was less than 1 m even in Sendai, which went up more than 4 km from the shoreline.

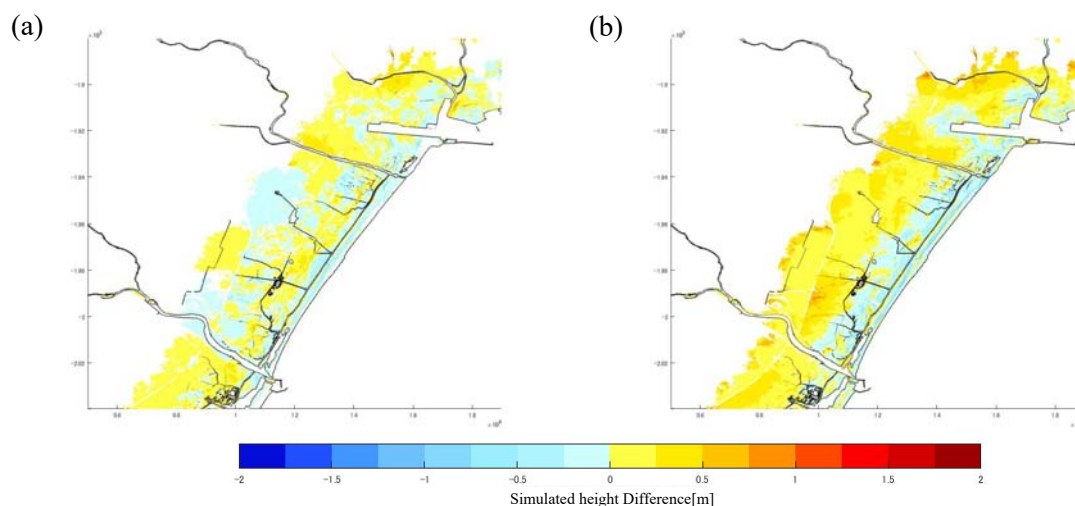


Fig. 8 – (a) Difference between "simulated height of roughness map" - "simulated height of roughness  $n = 0.025$ " (b) Distribution of difference between "simulated height of roughness  $n = 0.035$ " - "simulated height of roughness  $n = 0.025$ " in the TU model.



#### 4.4 The spatial grid resolution

The comparison of the spatial grid resolution was performed using the TU model and the FS model two type of the fault models for the results of  $\Delta x = 5$  m and 15 m. The roughness coefficient was set to 0.025 in the whole area.

When the grid resolution was changed to rough, the inundation height increased and the inundation area expanded in the two type of the fault model. (Fig. 9) However, this tendency depended on the location. Interestingly, the area where the inundation height changed largely was similar to the area where the two type of the fault model made largely different simulated heights at 5 m resolution as mentioned in section 4.2. The especially outstanding area were near the dikes on the south of the Nanakita River and the eastern Sendai road. Although the tsunami waveform was due to same fault model, the topography at 15m grid were smoothed compared to 5m grid. Therefore, the height of the Nanakita River dikes was low and the line discharge flux from the Nanakita River was increased. Regarding the eastern Sendai road, the almost disappeared waterway in Sendai plain at 15m grid made less tsunami decline in run-up process and the effect by the road embankment reflection increased.

Of course, in the area where the topography changes little by the grid resolution, the inundation height and area will hardly change. However, in Sendai, which has topography change in narrow area, the tsunami simulation need to be conducted at finer than 5m grid resolution.

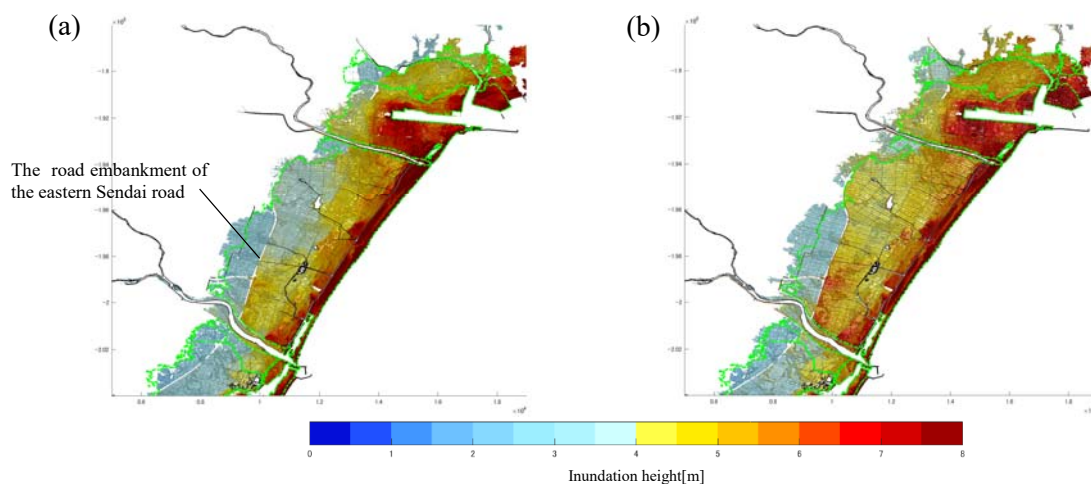


Fig. 9 – (a) Distribution of inundation height at 5 m simulation resolution in the TU model (b) Distribution of inundation height at 15 m simulation resolution in the TU model.

## 5. Conclusion

We compared with the traces collected after the 2011 Tohoku earthquake and evaluated how the change of the fault model and the roughness coefficient affected tsunami simulation. We used the trace data which were removed abnormally higher one than the surroundings, and the comparison was conducted with the trace heights comparable to tsunami simulation. Both of the two type of the fault models used in this study were overestimated. However, the distribution of the excessive simulated height tended to be different depending on the location of the trace, the reproducibility was good in coastal areas and bad in inland. In particular, in the area where the reproducibility was bad, some factors such as inflow from rivers or reflection from road embankment were confirmed to increase simulated height. This effect was greater than the that of roughness coefficients in the commonly used range. Also, the grid resolution of topography may increase the simulated height.



On the other hand, the number of traces used for comparing the simulated height was limited because of too wide inundation area or a few number of trace points due to the destructive tsunami. Therefore, we couldn't determine whether some local increase of the inundation height, such as the flow from the Nanakita River and the reflection by road embankment really occurred. To confirm these tsunami behavior, another approach, for example, analyzing the movie of tsunami recorded by fixed point camera and helicopter would help understanding tsunami run-up.

## 6. References

- [1] L. Montoya, P. Lynett, H. Thio, W. Li (2016): Spatial Statistics of Tsunami Overland Flow Properties, *J. of Waterway, Port, Coastal, and Ocean Engineering (ASCE)*
- [2] T. Baba, N. Takahashi, Y. Kaneda, K. Ando, D. Matsuoka, T. Kato (2015): Parallel Implementation of Dispersive Tsunami Wave Modeling with a Nesting Algorithm for the 2011 Tohoku Tsunami, *Pure appl. Geophys.*, **172**, 3455-3472
- [3] T. Tada, S. Nonaka, Y. Miyata (2018): Development of Tsunami Inundation Database Based on Post-Event Survey Results for Inundation Analysis, *Journal of Japan Society of Civil Engineers Ser. B1 (Hydraulic Engineering)*, **74**, I\_451-I\_456
- [4] C. Goto, Y. Ogawa, N. Shuto, F. Imamura (1997): *IUGG/IOC TIME Project, Numerical method of tsunami simulation with the Leap-frog scheme, UNESCO*
- [5] T. Takahashi (2004): Application of Numerical Simulation to Tsunami Disaster Prevention, *Journal of Japan Society of Computational Fluid Dynamics*, **12(2)**, 23-32
- [6] Y. Fujii, K. Satake, Y. Sakai, M. Shinohara, T. Kanazawa (2011): Tsunami source of the 2011 off the Pacific coast of Tohoku Earthquake, *Earth, Planets and Space*, **63**, 815-820
- [7] F. Imamura, Y. Koshimura, Y. Akita, Y. Nitta (2011): Implementation of the tsunami simulation for the 2011 Tohoku earthquake (Version1.1).  
[www.tsunami.civil.tohoku.ac.jp/hokusai3/J/events/tohoku\\_2011/model/dcrc\\_ver1.1\\_111107.pdf](http://www.tsunami.civil.tohoku.ac.jp/hokusai3/J/events/tohoku_2011/model/dcrc_ver1.1_111107.pdf)
- [8] The 2011 Tohoku Earthquake Tsunami Joint Survey (TTJS) Group (2011): <https://coastal.jp/ttjt/>
- [9] M. Kotani, F. Imamura, N. Shuto (1998): Tsunami run-up simulation and damage estimation by using GIS, *Proceedings of Coastal Engineering, JSCE*, **45**, 356-360
- [10] I. Aida (1977): Paleo-tsunami simulation along Sanriku-Oki. *Bulletin of the Earthquake Research Institute*, **52**, 71-101.
- [11] Japan Society of Civil Engineers (2002), Tsunami Assessment Method for Nuclear Power Plants in Japan (English Ver.), *JSCE*, 30.